Floating Conditions of the Pads in Fluid Pivot Journal Bearing

Vu Nguyen Tuyen (nguyentuyenvuvn@yaoo.com)
South China University of Technology https://orcid.org/0000-0003-4955-3207
Weiguang Li
South China University of Technology

Original Article

Keywords: fluid pivot bearing, floating conditions, optimal recess area

Posted Date: June 19th, 2020

DOI: https://doi.org/10.21203/rs.3.rs-36101/v1

Floating Conditions of the Pads in Fluid Pivot Journal Bearing

Nguyen Tuyen Vu*, Weiguang Li

Abstract

Fluid pivot journal bearing (FPJB) used on the ships was selected as the object of the study in this paper. The ability to form a squeeze film following the recess area ratio of the pad is systematically investigated under the condition that the preload factor and the eccentricity ratio change. Three positions of the load's characteristic for the moving conditions of boats on the water are considered. Numerical methods are used to calculate the dynamic lubrication in bearing. Equilibrium conditions of force and moment are used to determine the floating conditions of the pads. The results show that during working process, the pad directly applied by the external force satisfies the floating condition, while the remaining pads are satisfied only when the preload factor and eccentricity ratio increase. In the early stages, the pad mostly float on one side. Floating condition curves are constructed as the basis for determining the optimal recess area.

Keyword: fluid pivot bearing, floating conditions, optimal recess area.

1 Introduction

The tilting-pad journal is widely used in industry due to their excellent stability. Since created, it has shown to be superior to previous types of bearings. The tilt motion around the pivot of a pad is independent from the others, reducing vibration of the bearing better. The first version to be designed was mechanical pivot. Due to sliding motion, the mechanical pivot is abraded, creating a gap, which affects the accuracy and

*Correspondence: nguyentuyenvuvn@yaoo.com

School of Mechanical and Automotive Engineering, South China University of Technology.

operation of the bearing. Subsequently, the flexure pivot was investigated to overcome the wear in traditional pivot. In order to increase bearing stability, flexure pivot has been combined with squeeze film damper which has excellent damping properties but requires complex manufacturing technology.

Another method to increase the damping effect of bearings is to use squeeze oil film damper. This structure is simple, small-sized and easy to produce, so it is applied more and more widely in industry. So far, there have been many projects focusing on issues related to squeeze film such as vibration reduction effect of squeeze film, characteristics affecting the vibration reduction effect of squeeze film, optimizing squeeze film damper, ...[1-6] .

Combining tilting-pad journal bearings with simple squeeze film dampers will create a bearing that effectively reduces vibration. In 1977 a new tilting-pad bearing was introduced, called a fluid pivot bearing. During operation of the bearing, two regions of oil film will be formed: Hydrodynamic pressure oil film forms between the shaft and the inner surface of the pad; about 10% of lubricant from hydrodynamic pressure area flows through the gap into the recess, forming hydrostatic pressure. Research results show that fluid pivot bearing has better dynamic and static performance than mechanical pivot, systems using fluid pivot bearing have very good stability. The simple structure and manufacturing technology are the advantages that make it possible to be used in civil industry. At present, research results on this kind of bearing have not been published much. 1989, Nelson and Holling - sworth[7] used experiments and analysis to verify the basic principle of operation of Fluid Pivot journal bearings. Especially, the pressure in the recesses in the pads is considered according to the variation of applied load, the equilibrium position of the shaft according to the eccentricity ratio is also indicated. Harangozo, A.V[8] studies the stable performance of high-speed rotors using fluid-pivot and squeeze-film damper bearings. By using a simple model, he presented a significant

damping effect when using this type of bearing. LW Hollingsworth[9, 10] previously had also proposed a form of fluid pivot bearing which combines a squeeze oil film and flexible pads. However, this was not a self-generated squeeze oil film, but a static squeeze film created from an external device. Mingyang Lou[11] studied on the performance of fluid pivot journal bearing in one-sided state using experiments and numerical methods. The floating state of the pads was considered according to the shaft rotation speed and the the gap's diameter.

In order to reduce rotor amplitude transmitted to other components of the machine through bearing, many designs and technical solutions have also been studied. Santos on the basis of tilting-pad bearing has proposed active control method with rotor-bearing system[12, 13]. In these designs, high pressure nozzles are used to pump the oil directly into the gap between the bearing and the shaft. This high pressure oil flow is controlled by PI, PID feedback circuit and electrohydraulic servo valve. Therefore, the oil pressure will be distributed in the bearing properly and reduce the vibration of the shaft. The development trend of tilting-pad journal bearing with controllable lubrication is shown in the papers [14, 15]. Compared to these methods, fluid pivot bearing (with self-generated squeeze film) has a simpler structure and is much easier to implement. However, the biggest difficulty to a fluid pivot bearing is the condition of forming the squeeze film. Calculating, designing and ensuring the floating pad when operating are very important issues. Like in bearings that contain pads, determining the working characteristics for the pads should not be ignored. ZHU Aibin[16] and Wang, Y. L [17] systematically studied the swing characteristics of tilting pad bearing, considering factors affecting the swing characteristics of the pad. According to the knowledge of this paper's author about fluid pivot bearing, studies of floating conditions of pads are virtually not reported.

Fluid pivot journal bearing has good stability and capability of noise reduction due to

the hydrostatic and hydrostatic pressure oil film which is formed when the shaft rotates. These are great advantages for FPJB to be used on boats, aimed at reducing the impact on sailors' health. When moving on the sea, ships will be affected by waves, wind and other disturbances that make ships frequently swing. This swing causes variations in the direction and magnitude of the external forces affecting on the bearings. The change in the direction of the load can be simplified to the two working conditions shown in Figure 1.

Squeeze oil film formed during the bearing's operation is the distinct characteristic of this kind of bearing. Despite of having high damping effect and relatively simple structure, this type of bearing has not been widely applied because of its possibility to form squeeze oil film. If the pad does not float, the FPJB is similar to a multi-lobed. When recess area is large, the pad is easier to float, but the squeeze oil film's damping effect is reduced. So determining the optimal recess area is also the content needed to be done. From this fact, this work investigates the conditions of forming the squeeze oil film for bearings following the motion of the ship.

2 Numerical model and motion characteristics of the pad

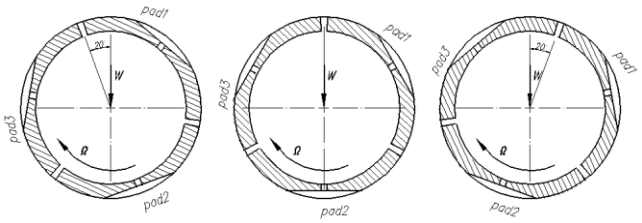

Figure 1 Three positions of load applying to the bearing when the ship oscillates

Geometry of FPJB and coordinate system is shown in Figure 2a. According to the FPJB's operation principle, two pressure zones will be formed when the shaft rotates: Hydrostatic pressure area is formed between the shaft and the inner surface of the pad; hydrostatic pressure at the recess. Reynolds equation governing the steady, laminar incompressible flows is given as follows:

In hydrodynamic oil film in dimensionless form:

$$\frac{\partial}{\partial\phi}\left(H_d^3\frac{\partial P_d}{\partial\phi}\right)+\left(\frac{D}{L}\right)^2\frac{\partial}{\partial\lambda}\left(H_d^3\frac{\partial P_d}{\partial\lambda}\right)=\frac{\partial H_d}{\partial\phi} \quad (1)$$

$$\frac{\partial}{\partial\phi}\left(H_s^3\frac{\partial P_s}{\partial\phi}\right)+\left(\frac{D}{L}\right)^2\frac{\partial}{\partial\lambda}\left(H_s^3\frac{\partial P_s}{\partial\lambda}\right)=0 \quad (2)$$

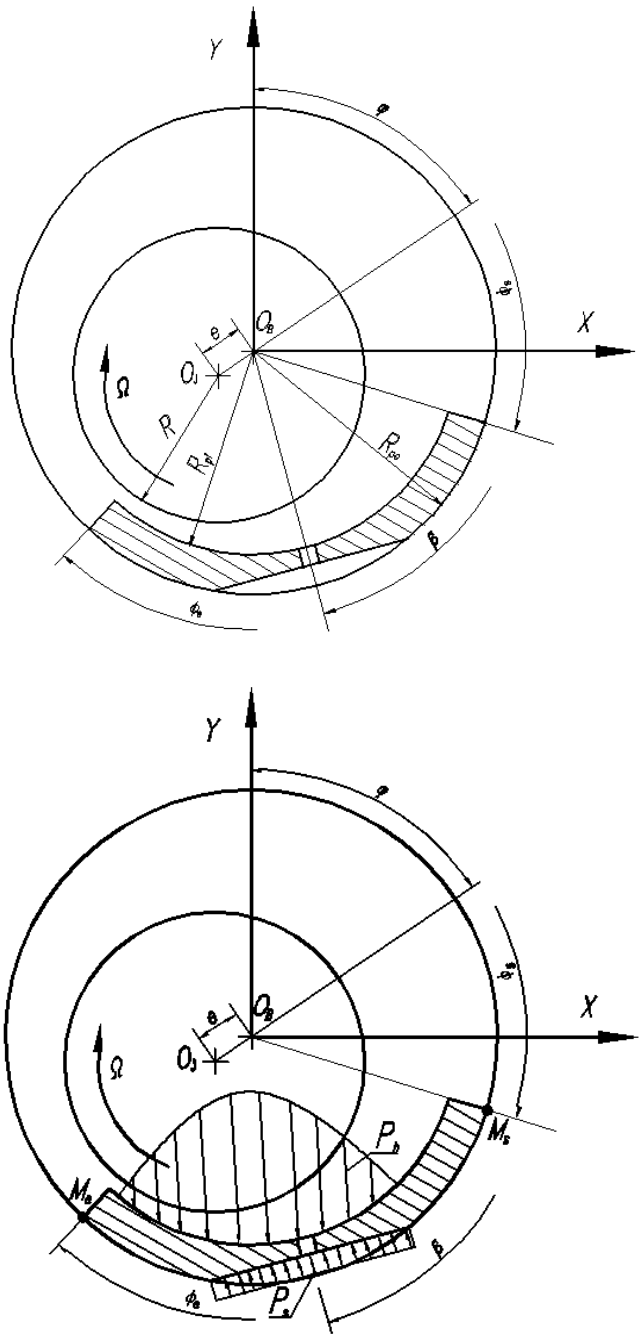

Figure 2 Fluid pivot bearing model

And in hydrostatic oil film in dimensionless form:

Where, H_d, H_s, P_d, P_s are dimensionless hydrodynamic oil film thickness, dimensionless hydrostaic oil film thickness, dimensionless hydrodynamic pressure,dimensionless hydrostatic pressure, respectively, ϕ, λ are angle measured from the horizontal split axis in the direction of rotation and coordinate in the axial direction, D, L are bearing diameter and bearing length.

When the pad has not floated (squeeze oil film has not been formed) static pressure in the recess will be equal to the hydrodynamic pressure at the gap. Hydrostatic pressure plays the role as a force that makes the pad float, while hydrodynamic pressure acts as a force preventing the pad from floating. When the pad begins to float, it will do one of two movements: 1. Translational movement in radial direction; 2. Rotational movement around a certain point. In case of rotational movement, because the outer surface of the pad initially comes into contact with the inner side of the bearing body, the pad

will float in one-sided at the beginning of floating state. This one-sided floating motion is also demonstrated in the paper [11].

The dynamics model of the pad is shown as in Figure 2, the equation of the pad's motion in the radial direction (Ignoring the effect of gravitational acceleration on the pad):

$$m_p \frac{dv}{dt} = F_s - F_d \tag{3}$$

$$m_p \frac{dv}{dt} = P_s A_{rf} - \int_{-1}^{1}\int_{\phi_s}^{\phi_e} P_d .d\lambda .d\phi \tag{4}$$

Rotational motion of the pad:

$$J_p \frac{d^2\theta}{dt^2} = M_s - M_d \tag{5}$$

Here,

$$M_s = P_s A_{rt} R_{po} \sin(\beta - \phi_s) \tag{6}$$

$$M_d = R_{po} \int_{\phi_s}^{\phi_e}\int_{-1}^{1} P_d \sin(\phi_s - \phi) d\lambda d\phi \tag{7}$$

Where, m_p, J_p are mass and moment of inertia of pad, F_d, F_s are force of hydrodynamic pressure and hydrostatic pressure, M_d, M_s are torque of hydrodynamic pressure and hydrostatic pressure, dv/dt is acceleration of pad, A_{rf} is recess area, θ is tilting angle, ϕ_s, ϕ_e are position angle of pad start and end edge, β is pad arc, R_{po} is radius of curvature of the outer surface of the bearing pad.

In order to have the pad floated, the force and moment applying on the pad have to satisfy either case $F_s > F_d$ or $M_s > M_d$.

3 Results and discussions

In order for the pad to float, the oil pressure in the recess must first exist, it means that there must be hydrodynamic pressure at the position of the gap. In fluid pivot bearing, gaps are created at the geometric center of the pads. Thus, in order for the pad to float, the pre-acquisite condition is that hydrodynamic pressure has to be formed on the pad, and this hydrodynamic pressure must appear in the geometric center of the pads. Second, this pressure must be large enough to exert pressure on the recess to form the force and the hydrostatic moment overpowering the hydrodynamic force and moment. With each value of the hydrodynamic pressure at the gaps (parameters m, ε, φ,… have been determined), the

size of the recess area determines the possibility of forming the squeeze-film.

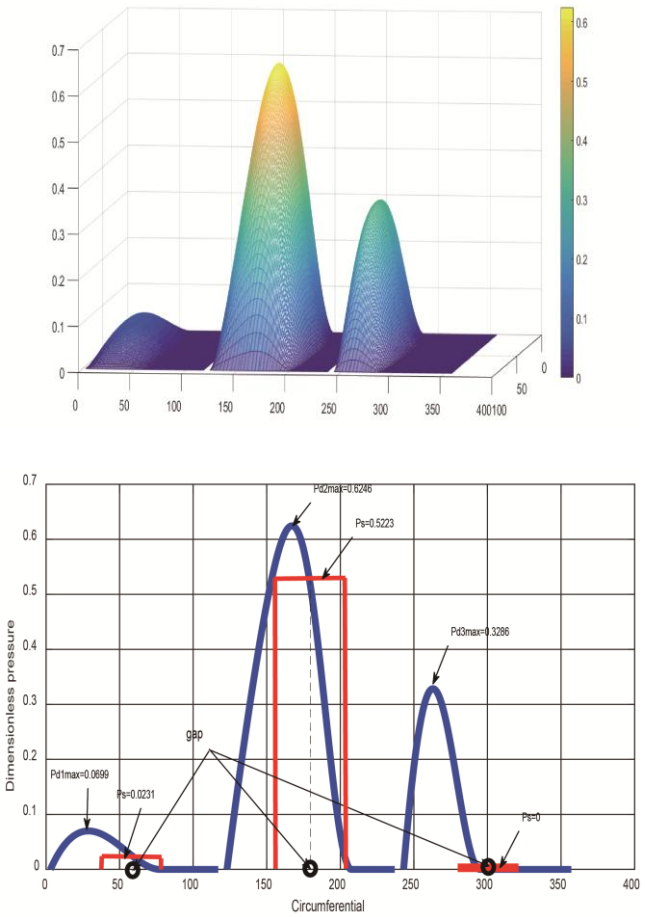

Figure 3 Hydrodynamic and hydrostatic pressure distribution on the pads and

Figure 3 shows the hydrodynamic and hydrostatic pressure distribution on the pads and in the recesses. It can be clearly seen that in this case the squeeze oil film definitely forms on pad2, on pad1 it is very difficult to form (if formed, the recess area is very large) and on pad3 it will not be able to form a squeeze oil film.

Table 1 Specification of the bearing

Parameters	Value [unit]
Journal radius (R)	100 [mm]
Bearing length (L)	150 [mm]
Number of pads (N_p)	3
Radius of curvature of the inner surface of the bearing pad (R_i)	100,21 [mm]
Radius of curvature of the outer surface of the bearing pad (R_o)	115[mm]
Pad arc (β)	114[deg]
Position angle of pad manufacture center	60, 180, 300[deg]

In order to determine the floating conditions for the pad, the calculation steps are conducted as follows:

1. Determining the parameters of bearings (These parameters are shown as in Table 1);

2. Calculating the equilibrium for the shaft-bearing system with preload factors (m=0.1, 0.3,

0.5, 0.7, 0.9), from there, the hydrodynamic pressure and the pressure at gap are determined;

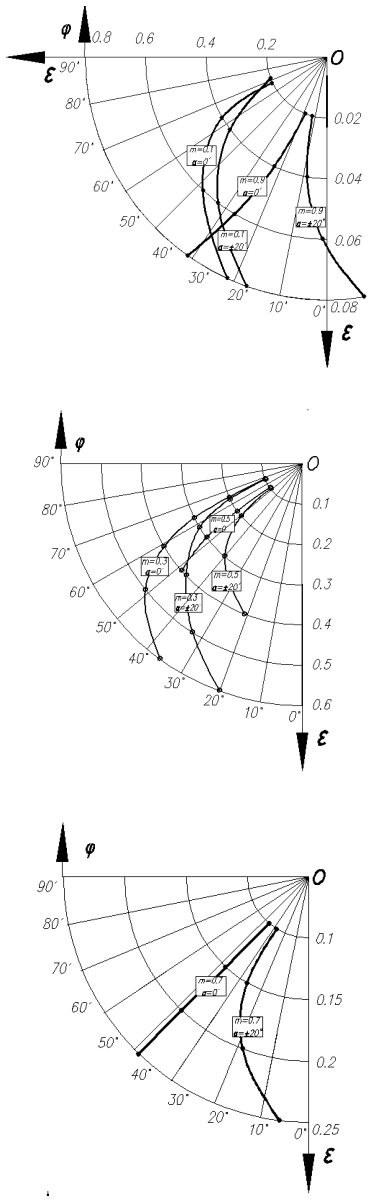

Figure 4 The equilibrium position of the shaft

3. Based on equations 1, 2, 3, 4, 5 determining the recess area required for the pad to float.

The equilibrium of the journal center in the bearing is shown as in Figure 4. The attitude angle in case $\alpha=0$ is greater than that of the case $\alpha=\pm 20^0$.

3.1 Preload factor m=0.1

In all 3 cases ($\alpha = 0$, $\alpha = \pm 20$) the pads 2 always satisfy floating conditions, the pads 3 does not satisfy any floating conditions (most on the pad3 do not form oil film pressure). The pads1 has floating conditions existed but not with every position of the shaft. In most cases, the moment curve (blue) is lower than the force curve, indicating that the pad is easier to float on one side. Only in the case of $\varepsilon>0.33$ and $\alpha = 0$ the pad2 will move following the radial direction instead of tilting to one side.

The variation rule of the "recess area ratio" is different from the "eccentricity ratio" in these 3 cases. In case of $\alpha = 20$ (Figure 5a), when the eccentricity ratio increases to 0.6, the squeeze oil film on pad2 is easier to be formed and vice versa. On pad1, when the eccentricity ratio increases, the squeeze-film becomes harder to be formed. In

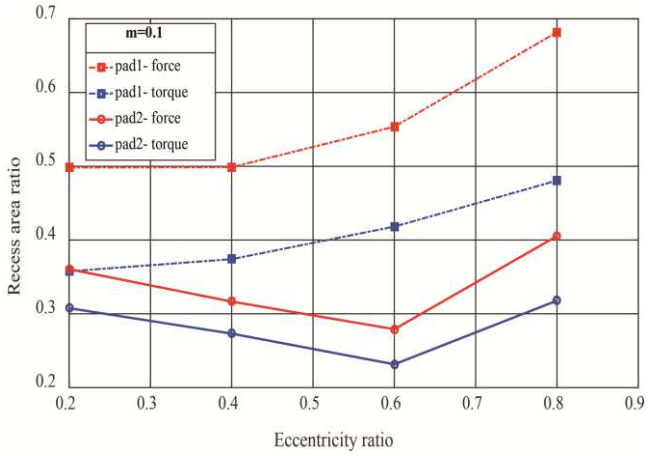

a. $\alpha=20^0$

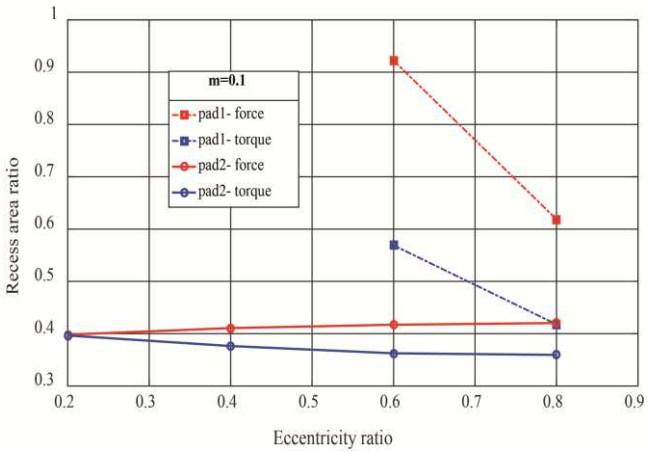

b. $\alpha=-20^0$

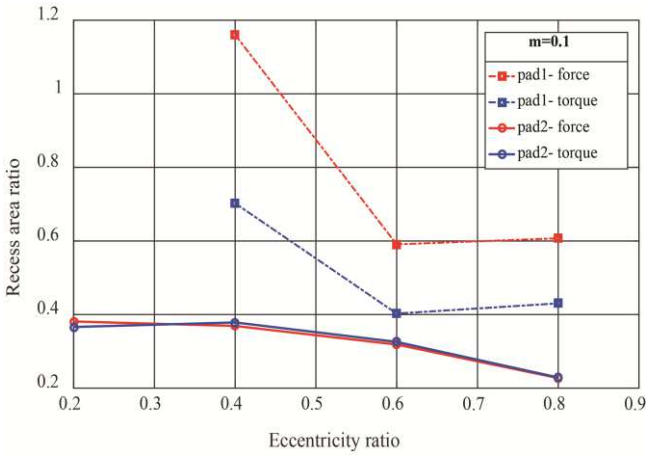

c. $\alpha=0$

Figure 5 Floating conditions of the pads when preload factor m=0.1

case of $\alpha = 0$ (Figure 5c), if the eccentricity increases, the pad2 will float more easily. The pad1 can only float when $\varepsilon > 0.4$: within $0.4 < \varepsilon < 0.6$ the increase in eccentricity will make the pad easier to float and vice versa. In case of $\alpha = -20$ (Figure 5b), both pad1 and pad2 are easy to float when the eccentricity ratio increases. For pad2, the ability of floating varies due to variation of the force and moment applying on the pad. According to Figure 5, to ensure that the pressed oil film is able to be formed on pad2, the recess area ratio (Λ) $\Lambda > 0.4$.

3.2 Preload factor m=0.3

Calculation results are shown in Figure 6. In all 3 cases, the pad2 satisfy floating conditions, and hydrodynamic film pressure has been formed on the pad3. However, this oil film does not exist in the gap on the pad so the pad3 can not float.

Figure 6a shows the conditions for forming the squeeze film in case $\alpha = 20^0$. In this case, both pad1 and pad2 float with every position of the shaft center. At two positions corresponding to ε_{max} and ε_{min}, both pads are

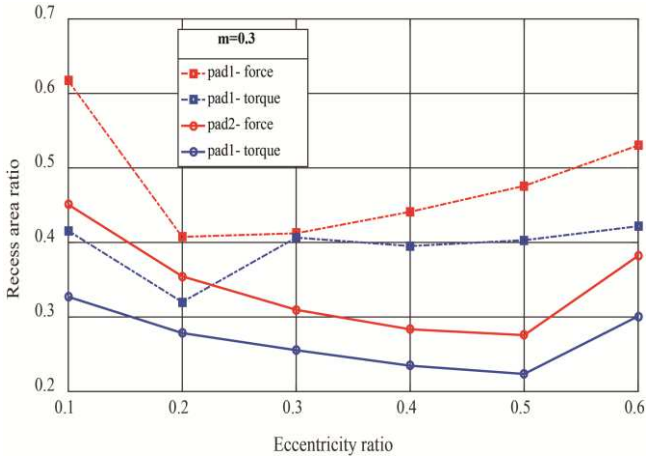

a. $\alpha=20^0$

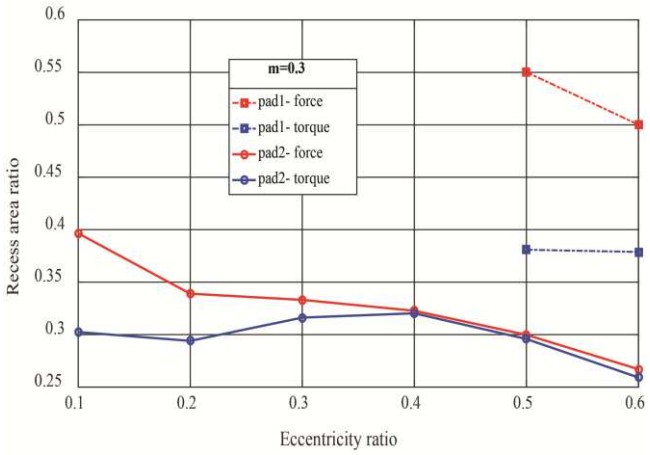

b. $\alpha=-20^0$

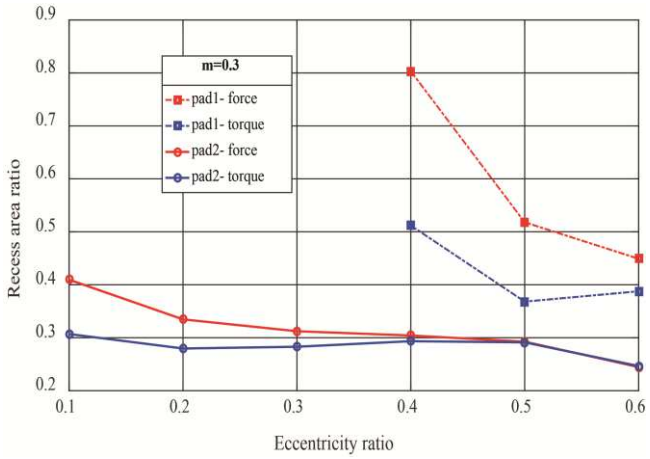

c. $\alpha=0$

Figure 6 Floating conditions of the pads when preload factor m=0.3

most difficult to float. Pad1 is most floatable at $\varepsilon \approx 0.2$, whereas pad2 is best at $\varepsilon \approx 0.5$. In case $\alpha=0^0$ (Figure 6c), the two positions that pad2 is easiest to float are at $\varepsilon \approx 0.2$ and $\varepsilon \approx 0.6$. $\varepsilon \approx 0.1$ and $\varepsilon \approx 0.5$ are the two positions that pad2 is most difficult to float. Pad1 starts to float with $\varepsilon \approx 0.4$, $\varepsilon \approx 0.5$ is the position where the pad is most floatable. In case $\alpha=-20^0$ (Figure 6b), the shape of the pad2's moment curve is similar to that in case $\alpha=0$. $\varepsilon \approx 0.2$ and $\varepsilon \approx 0.6$ are two positions where pad2 is most floatable. It is most difficult of the pad2 to float at $\varepsilon \approx 0.4$. Pad1 can float only when $\varepsilon \approx 0.5$. This is the case where pad1 most difficultly float. The bigger ε is, the more easily pad1 can float. In order to have pad2 constantly floated , then $\Lambda \geqslant 0.327$.

3.3 Preload factor m=0.5

At the value of this preload factor, both pad1 and pad2 completely satisfy the floating conditions. However, there is still no position where pad3 satisfies conditions for forming squeeze film. For case $\alpha = 20^0$, the shape of the curves of pad1 and pad2 are the same, and similar

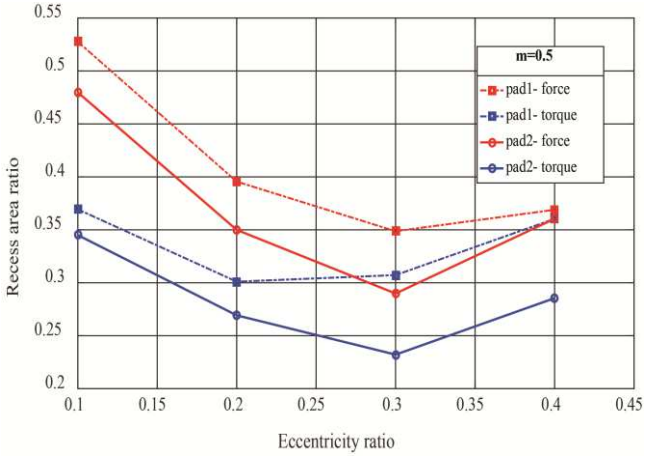

a. $\alpha=20^0$

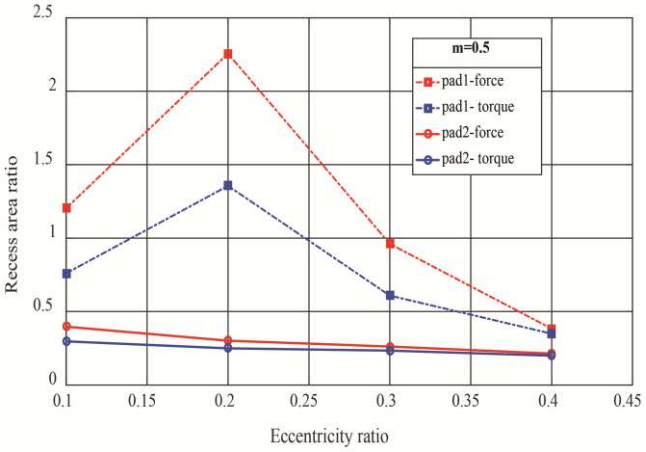

b. $\alpha=-20^0$

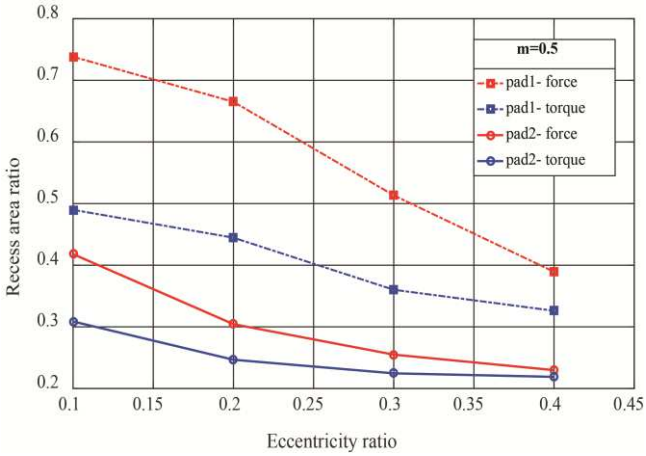

c. $\alpha=0$

Figure 7 Floating conditions of the pads when preload factor m=0.5

to the curve of pad2 (m = 0.3, α = 20). ε has lowest value when the pad most difficultly float. The floating condition of the pad increases when ε reaches approximately 0.3. Subsequently, squeeze film is harder to be formed when ε increases. With ε=0.1, a hydrodynamic oil film is formed at the center of pad3, but the pressure peak is too far away from the gap, so it cannot satisfy floating conditions (to float Λ>17.5).

In other positions, although hydrodynamic oil film is formed on the pad, it does not cover the gap. For α = 0, the variation law of Λ with the same value of ε for pad1 and pad2. The further away from the center of the bearing center, the easier the squeeze film can be formed. On pad3, a hydrodynamic pressure film is formed, but only when ε=0.1 is a hydrodynamic pressure formed at the gap area. However, the oil film pressure at the gap is not large enough to make pad3 float ($\Lambda \geqslant$ 4.8). In case α = -20, when ε increases, pad2 becomes more and more floatable. While the floating ability of pad1 initially decreases, it then increases. On the pad3, hydrodynamic pressure

has been formed but at the gap's position, this pressure is not formed. So that, the pad3 does not satisfy floating conditions. Conditions for pad2 to have the squeeze film constantly formed: Λ> 0.345.

3.4 Preload factor m=0.7

Pad1 has satisfied floating conditions with every position of load and eccentricity ratio. According to Figure 8, we can see that the variation law of the floating conditions for pad1 is the same in the three positions of the external force. The bigger the eccentricity ratio ε is, the easier for it to float. Λ>0.334 is the condition for pad1 to always float when the bearing is working.

The floating conditions of pad2 are well satisfied. The shapes of the curves are the same when the value of m = 0.5 (corresponding to 3 cases α = 0, ± 20). The floating condition for pad2 when the bearing is operating is Λ> 0.64.

Pad3 is still not able to satisfy floating conditions when the bearing is working, although the hydrodynamic pressure film has been formed

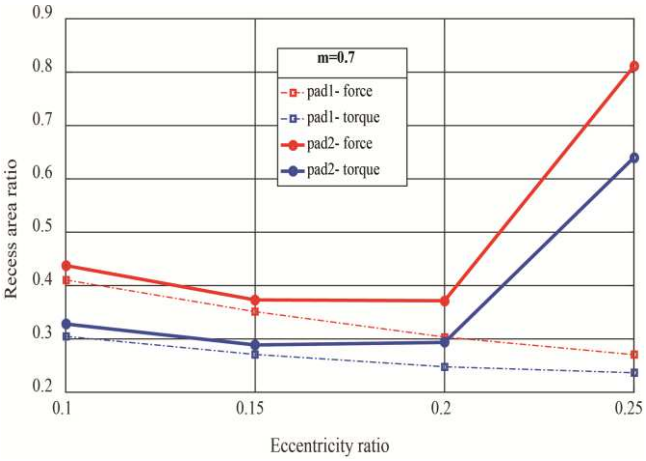

a. α=20^0

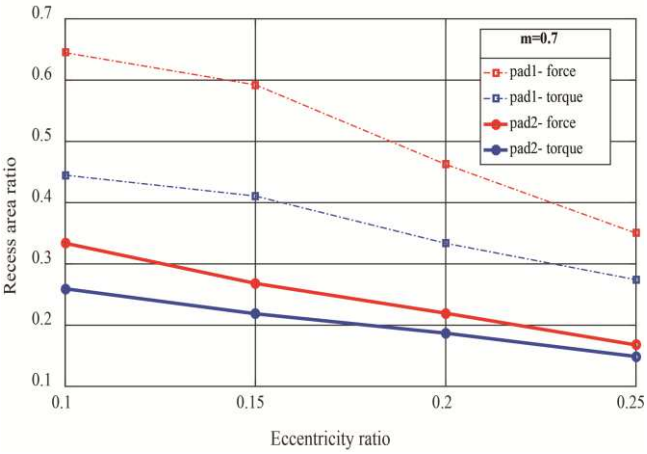

b. α=-20^0

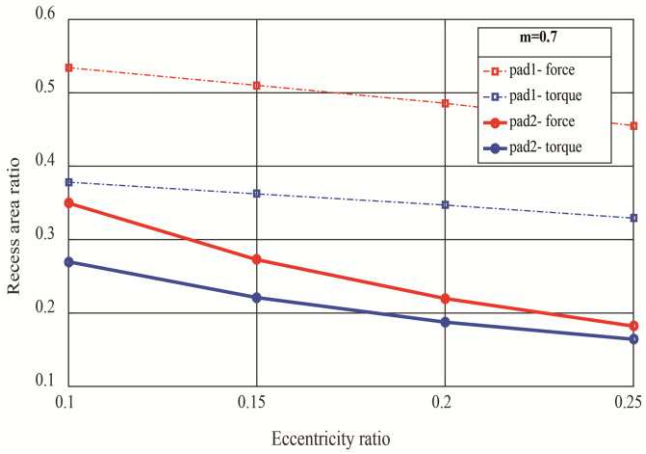

c. α=0

Figure 8 Floating conditions of the pads when preload factor m=0.7

on the pad. Even with some positions of the shaft center, the hydrodynamic pressure has been formed on the pad, but its value is not large enough. Specifically, where α = 20 at position ε = 0.1, Λ> 2.46 is the floating condition of the pad3. In case of α = 0, the floating condition of pad3 when ε = 0.1 is Λ> 2.25 and when ε = 0.15, it is Λ> 107. In case of α = -20, when ε = 0.1 and 0.15, the floating conditions are 17307 and 25, respectively.

3.5 Preload factor m=0.9

The result of Figure 9 shows that with this preload value, the floating conditions of all 3 pads are completely satisfied. The relationship of recess area ratio and eccentricity ratio on pad1 and pad2 is basically the same as when the preload factor m = 0.7. Only when α=0, floating conditions pad1 are almost unchanged. The squeeze film is formed on pad3, but when ε is large, it is more difficult to form this oil film. The conditions for pad1 and pad2 to float completely during the bearing's operation are 0.29 and 0.28 respectively. When bearing operates, there is a

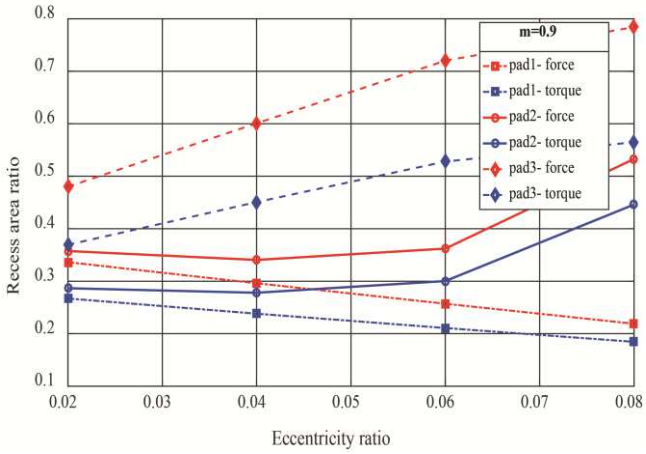

a. $\alpha=20^0$

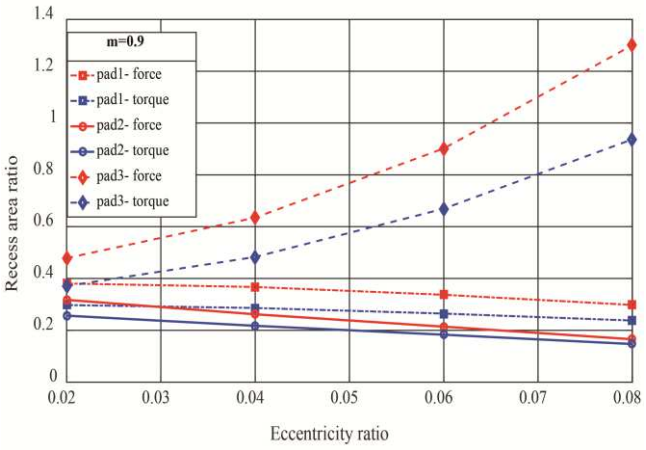

b. $\alpha=-20^0$

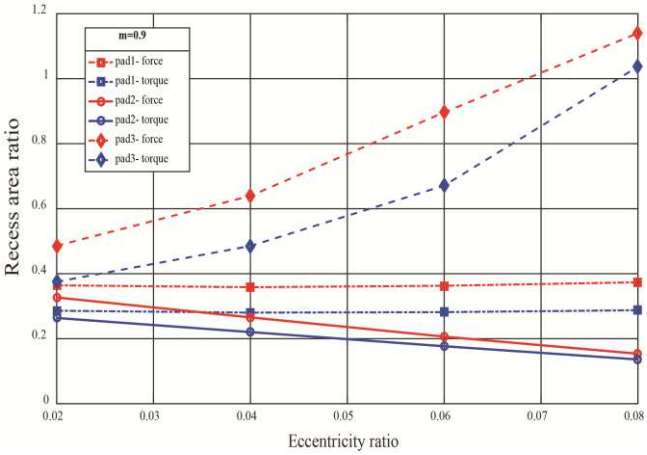

c. $\alpha=0$

Figure 9 Floating conditions of the pads when preload factor m=0.9

period of time during which the pad 3 cannot float.

4 Conclusions

The paper have constructed mathematic models and used numerical methods to determine the floating conditions for the pad in conditions of ships moving on the water. Based on the obtained results, some conclusions can be withdrawn:

(1) The floating condition of the pad (start-up phase) depends only on the bearing structure (mainly the pad structure) and does not depend on the rotation speed of the shaft and the oil viscosity.

(2) The moment curve is always lower than the force curve. This result shows that in the early stages the pad will be in one-sided floating state.

(3) The ability to form squeeze oil film increases as the preload factor increases. The squeeze oil film is best formed on pad2, then pad1 and finally pad3. With low preload factor, pad3 does not have a hydrodynamic film formed. When the preload factor m increases, the hydrodynamic pressure is gradually formed on pad3 but not the squeeze oil film. When m = 0.9 on pad3, it satisfies the condition of forming an oil film.

(4) The variation of direction of external force also greatly affects the floating conditions of the pad. In the case of α = 0 and α = -20, the higher the eccentricity ratio is, the easier for pad1 and pad2 to have squeeze oil film formed. In case of α = 20, the increase of eccentricity ratio will make the oil film pressing on pad1 easier to be formed, while on pad2, this ability initially increases, it then decreases. The floating condition of pad2 is most affected when the external force direction changes.

Authors' Contributions

Nguyen Tuyen Vu carried out the numerical simulation and manuscript writing. Weiguang Li read and approved the final manuscript.

Authors' Information

Nguyen Tuyen Vu, born in 1986. He is the Ph. D. candidate at the School of Mechanical and Automotive Engineering, South China University of Technology, China. He received the B.S, M.S. degrees in Mechanical Engineering from Le-Quy-Don Technical University, Viet Nam in 2011, 2016, respectively. From 20011 to 2017, he was a lecturer at Le-Quy-Don Technical University, Viet Nam. His research interest covers vibration control.

Weiguang Li(1958, Male), PhD, Professor and doctoral supervisor. He received the B.S, M.S. and Ph.D. degree in mechanical engineering from the Mechanical and Automotive Engineering, South China University of Technology, China in 1982, 1996, 1999, respectively. From 2001 to 2015, he was a director of the research of modern NC Technology, School of mechanical and automotive engineering. South China University of Technology. Vice President of Guangdong manufacturing information society, director of hardware products Standardization Technical Committee. His research interest covers modern CNC equipment, manufacturing system of digital and information control, industrial robot technology, electromechanical integration equipment, steam turbine bearing, and the shafting vibration monitoring, and vibration reduction technology. He has been more than 10 technical achievements in enterprise application and industrialization of new technologies for CNC machining center is to promote. Optical-mechanical-electrical integration results of the aviation industry, scientific and technological progress Award 1995, CNC technology, Guangdong Provincial Science and technology progress award of Guangdong excellent new product Award. He has won more than 30 national invention patent and utility model patents. In recent years, he has more than 100 papers published in national and international academic papers, editors published a modern manufacturing technology (mechanical industry publishing house), mechanical control Foundation (bilingual tutorial) (Wuhan University of

technology press), the machinery and equipment of CNC technology (national defense industry press) and 3 textbooks.

Competing Interests

The authors declare that they have no competing interests

Ethics Approval and Consent to Participate

Not applicable.

Funding

The support from National Natural Science Foundation of China(NSFC, Grant No. 51875205 and 51875216), the Natural Science Foundation of Guangdong Province
(Grant No. 2018A030310017), as well as the Science and Technology Plan Projects of Guangzhou from China
(Grant No.201904010133) for this research is gratefully acknowledged.

References

[1] J. V. Beck, and C. L. Strodtman, 1967, "Stability of a Squeeze-Film Journal Bearing," *Journal of Lubrication Technology,* vol. 89, 3, pp. 369-373.

[2] C. L. Strodtman, 1971, "Optimization of Clearance in a Squeeze-Film Journal Bearing," *Journal of Lubrication Technology,* vol. 93, 2, pp. 246-251.

[3] Y. Sato, H. Fujino, H. Sakakida, and S. Hisa, 1991, "Stability Characteristics of a Journal Bearing Mounted in an Uncentralized Squeeze Film Damper," *Journal of Tribology,* vol. 113, 3, pp. 584-589.

[4] L. S. Andres, 2014/03/01/, 2014, "Force coefficients for a large clearance open ends squeeze film damper with a central feed groove: Experiments and predictions," *Tribology International,* vol. 71, pp. 17-25.

[5] S.-H. Jeung, L. San Andrés, and G. Bradley, 08/06, 2015, "Forced Coefficients for a Short Length, Open-Ends Squeeze Film Damper With End Grooves: Experiments and Predictions," *Journal of Engineering for Gas Turbines and Power,* vol. 138.

[6] K. C. Choy, and J. D. Halloran, 1982/01/01, 1982, "Application of Hydrostatic Squeeze-Film Dampers," *A S L E Transactions,* vol. 25, 2, pp. 245-251.

[7] D. V. Nelson, and L. W. Hollingsworth, 1977, "The Fluid Pivot Journal Bearing," *Journal of Lubrication Technology,* vol. 99, 1, pp. 122-127.

[8] A. V. Harangozo, and T. A. Stolarski, 1993/12/01/, 1993, "Fundamental dynamic performance of fluid-pivot and squeeze-film damper bearings," *Tribology International,* vol. 26, 6, pp. 413-419.

[9] H. LW, 1970 Dec 22, " Hydrostatically supported tilting pad journal bearing," vol. 3.

[10] H. LW, 1977 Nov 22, "Hydrostatically supported tilting pad journal bearing improvements.," *Inventor; Pioneer Motor Bearing Co, assignee*, pp. 4(059):318.

[11] M. Lou, O. Bareille, W. Chen, and X. Xu, 2019/10/01/, 2019, "Experimental and numerical investigation on the performance of fluid pivot journal bearing in one-sided floating state," *Tribology International,* vol. 138, pp. 353-364.

[12] I. F. Santos, and F. H. Russo, 1998, "Tilting-Pad Journal Bearings With Electronic Radial Oil Injection," *Journal of Tribology,* vol. 120, 3, pp. 583-594.

[13] I. Santos, and A. Scalabrin, 01/01, 2003, "Control System Design for Active Lubrication With Theoretical and Experimental Examples," *Journal of Engineering for Gas Turbines and Power-transactions of The Asme - J ENG GAS TURB POWER-T ASME,* vol. 125.

[14] I. Santos, 01/01, 2011, "On the future of controllable fluid film bearings," *Mécanique & Industries,* vol. 12.

[15] I. Santos, "Trends in Controllable Oil Film Bearings," pp. 185-199, 2011.

[16] A. Zhu, Y. Yang, H. Xiao, and W. Chen, *Swing characteristic of pads in four-pad tilting pad bearing*, 2013.

[17] Y. L. Wang, Z. S. Liu, and D. S. Qian, 09/01, 2011, "Swing characteristic of pads in tilting pad bearing," *Harbin Gongye Daxue Xuebao/Journal of Harbin Institute of Technology,* vol. 43, pp. 62-66.

Figures

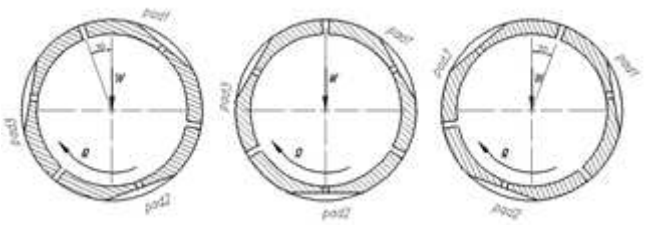

Figure 1

Three positions of load applying to the bearing when the ship oscillates

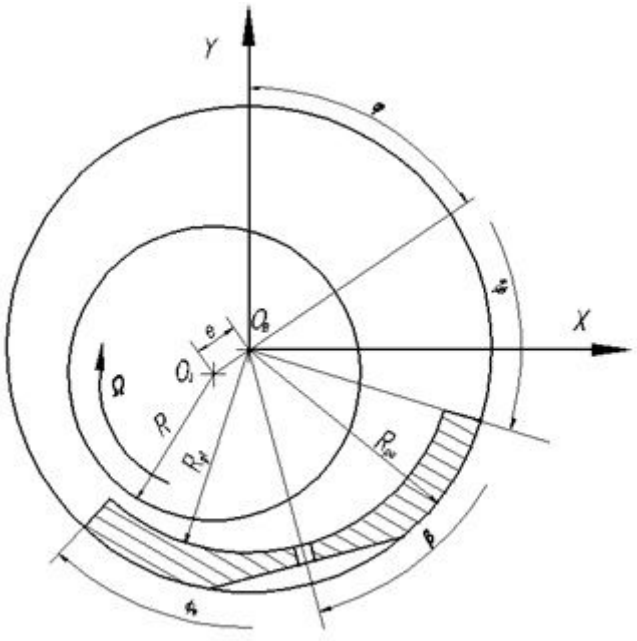

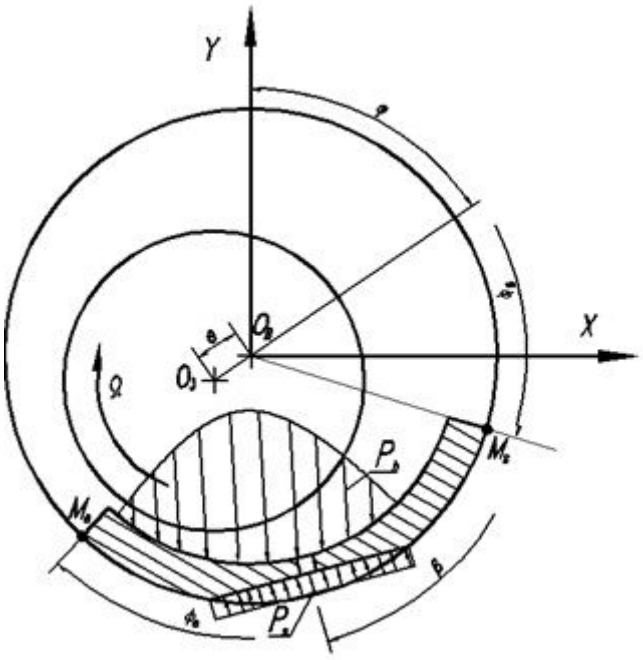

Figure 2

Fluid pivot bearing model

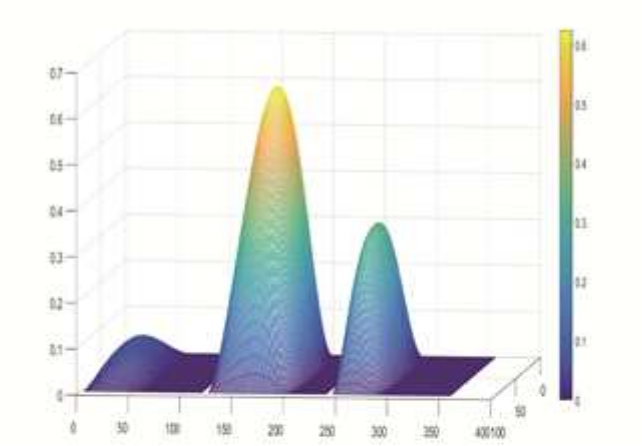

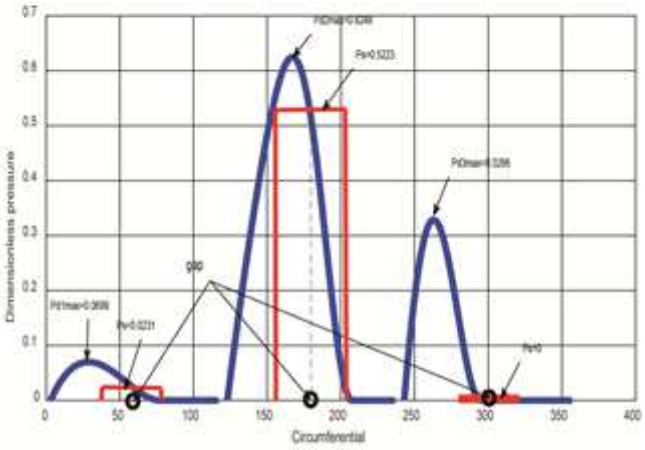

Figure 3

Hydrodynamic and hydrostatic pressure distribution on the pads

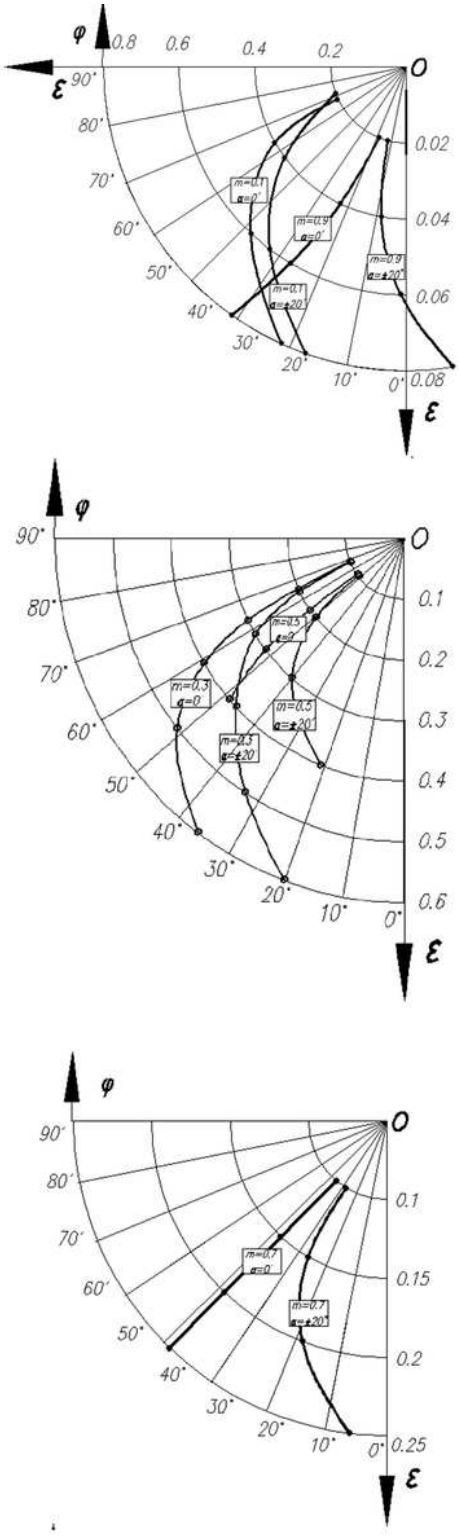

Figure 4

The equilibrium position of the shaft

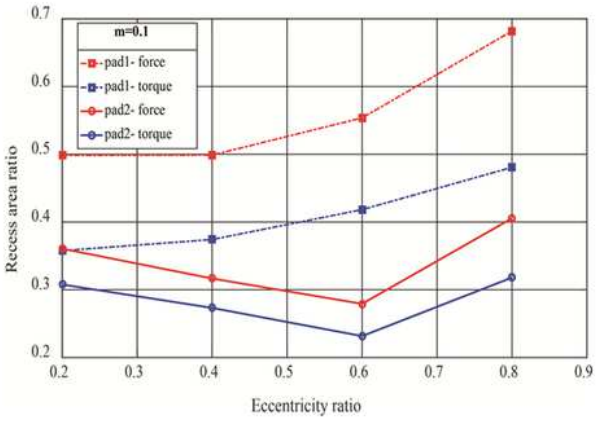

a. $\alpha=20^0$

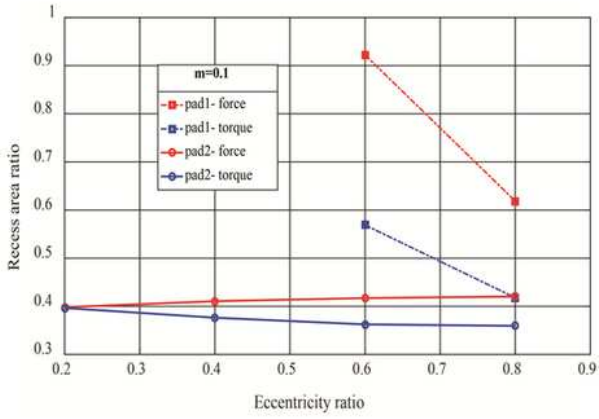

b. $\alpha=-20^0$

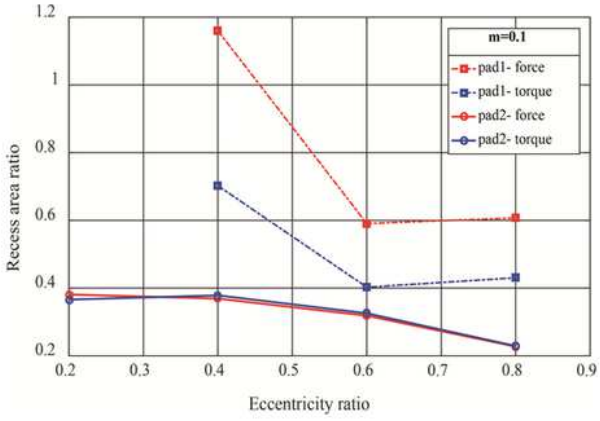

c. $\alpha=0$

Figure 5

Floating conditions of the pads when preload factor m=0.1

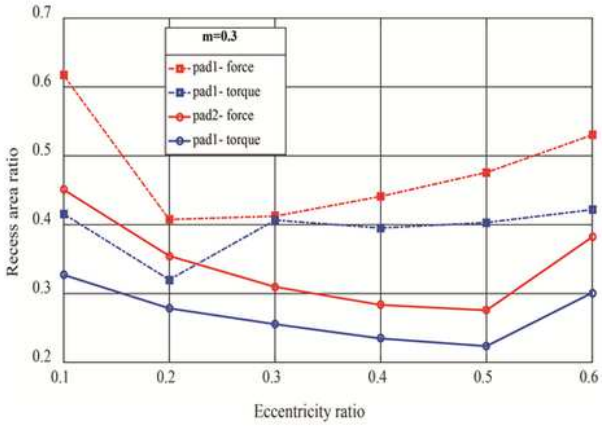

a. $\alpha=20^0$

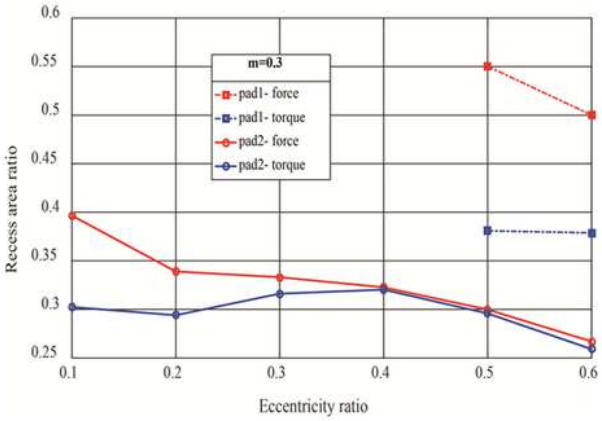

b. $\alpha=-20^0$

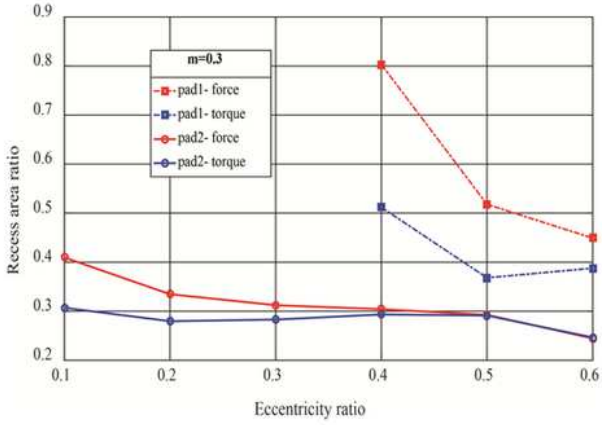

c. $\alpha=0$

Figure 6

Floating conditions of the pads when preload factor m=0.3

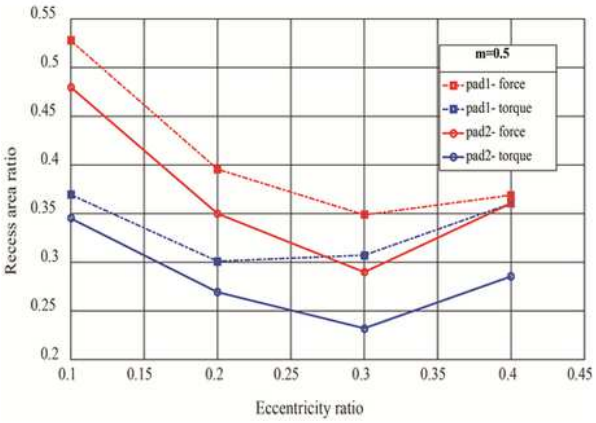

a. $\alpha=20^0$

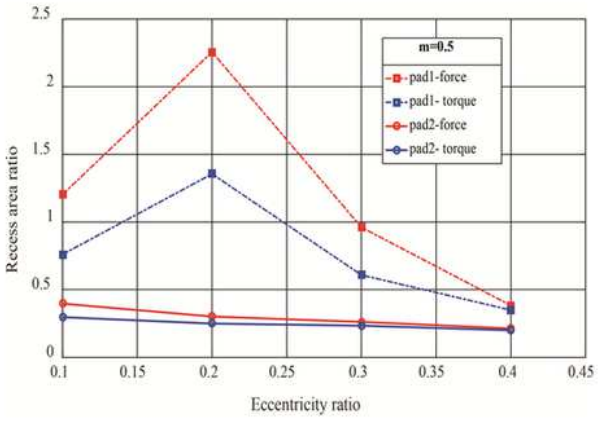

b. $\alpha=-20^0$

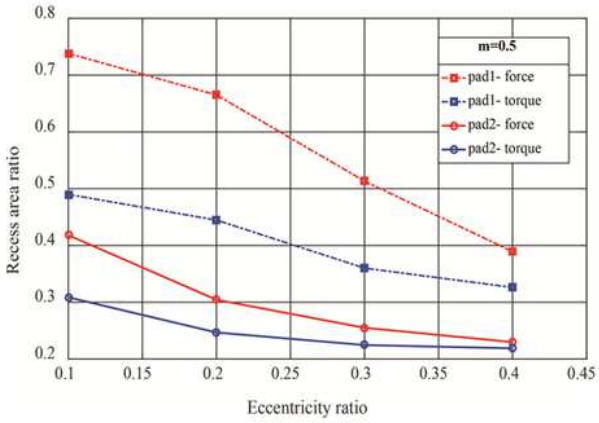

c. $\alpha=0$

Figure 7

Floating conditions of the pads when preload factor m=0.5

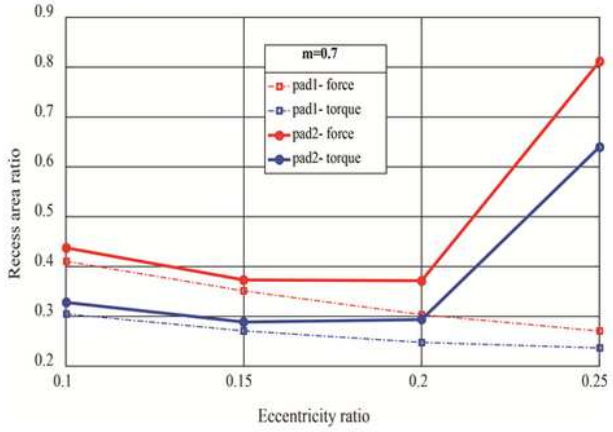

a. $\alpha=20^0$

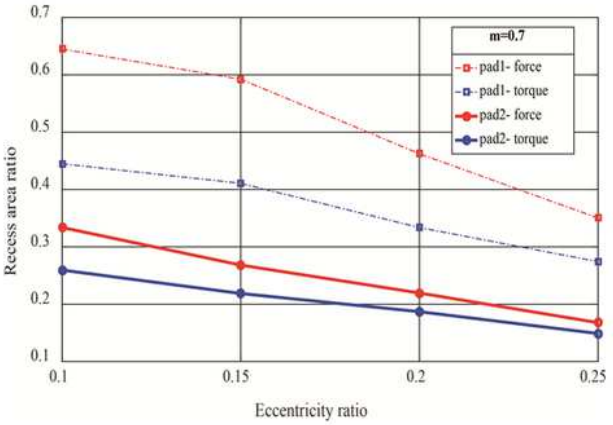

b. $\alpha=-20^0$

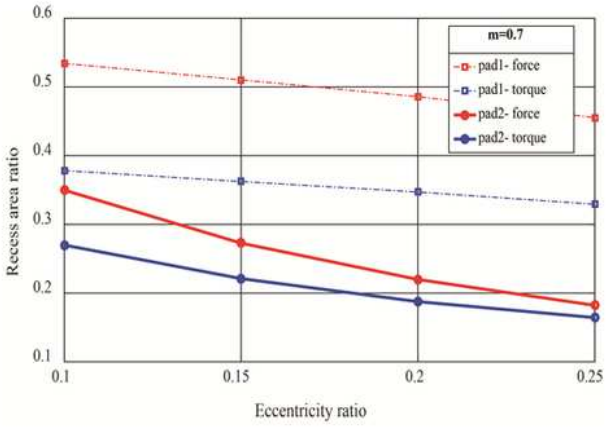

c. $\alpha=0$

Figure 8

Floating conditions of the pads when preload factor m=0.7

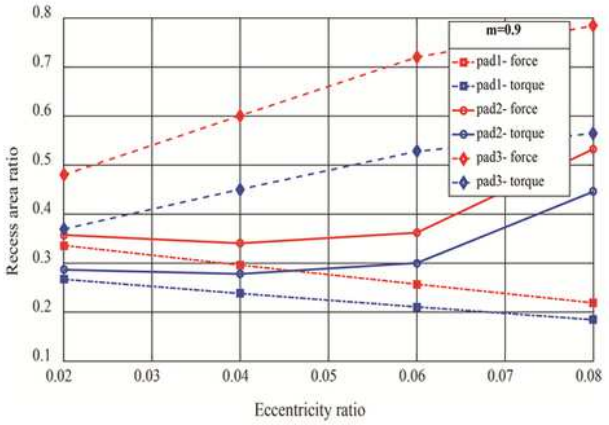

a. $\alpha=20^0$

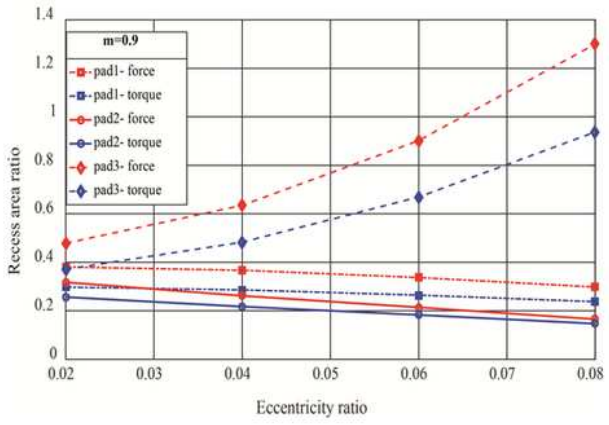

b. $\alpha=-20^0$

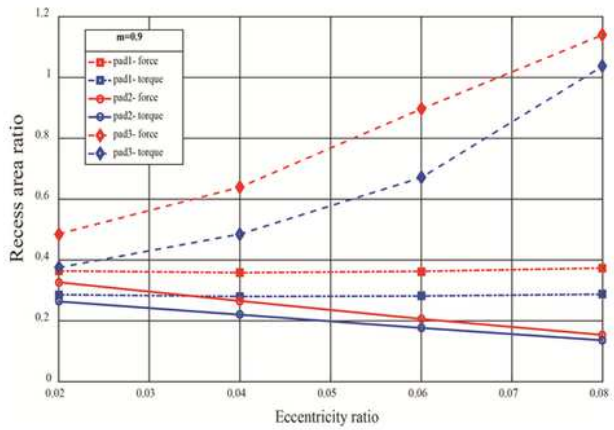

c. $\alpha=0$

Figure 9

Floating conditions of the pads when preload factor m=0.9